

Origins of nonzero multiple photon emission probability from single quantum dots embedded in photonic crystal nanocavities

Hsiang-Szu Chang, Wen-Yen Chen, Tzu-Min Hsu, Tung-Po Hsieh, Jen-Inn Chyi, and Wen-Hao Chang

Citation: *Applied Physics Letters* **94**, 163111 (2009); doi: 10.1063/1.3125222

View online: <http://dx.doi.org/10.1063/1.3125222>

View Table of Contents: <http://scitation.aip.org/content/aip/journal/apl/94/16?ver=pdfcov>

Published by the [AIP Publishing](#)

Articles you may be interested in

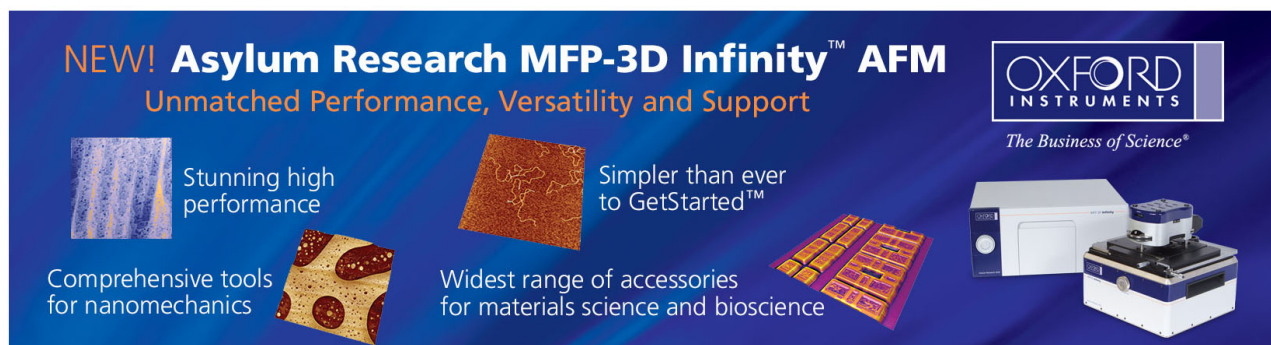
[Control of spontaneous emission from InP single quantum dots in GaInP photonic crystal nanocavities](#)
Appl. Phys. Lett. **97**, 181104 (2010); 10.1063/1.3510469

[Mode identification of high-quality-factor single-defect nanocavities in quantum dot-embedded photonic crystals](#)
J. Appl. Phys. **101**, 073107 (2007); 10.1063/1.2714644

[Enhancement and suppression of spontaneous emission by temperature tuning InAs quantum dots to photonic crystal cavities](#)
Appl. Phys. Lett. **88**, 131101 (2006); 10.1063/1.2189747

[Optical emission from individual InGaAs quantum dots in single-defect photonic crystal nanocavity](#)
J. Appl. Phys. **98**, 034306 (2005); 10.1063/1.1953885

[Enhanced spontaneous emission from InAs/GaAs self-organized quantum dots in a GaAs photonic-crystal-based microcavity](#)
J. Appl. Phys. **93**, 6173 (2003); 10.1063/1.1566470

The advertisement features a dark blue background with a grid of images showing various AFM scan results. The text is in white and orange. The Oxford Instruments logo is in the top right corner. The main headline is 'NEW! Asylum Research MFP-3D Infinity™ AFM' in white, with 'Unmatched Performance, Versatility and Support' in orange below it. The Oxford Instruments logo is in the top right corner, with the tagline 'The Business of Science®' below it. The advertisement highlights four key features: 'Stunning high performance' (with a scan image), 'Simpler than ever to GetStarted™' (with a scan image), 'Comprehensive tools for nanomechanics' (with a scan image), and 'Widest range of accessories for materials science and bioscience' (with a scan image). An image of the MFP-3D Infinity AFM system is shown in the bottom right corner.

Origins of nonzero multiple photon emission probability from single quantum dots embedded in photonic crystal nanocavities

Hsiang-Szu Chang,¹ Wen-Yen Chen,¹ Tzu-Min Hsu,^{1,a)} Tung-Po Hsieh,² Jen-Inn Chyi,² and Wen-Hao Chang³

¹Department of Physics and Center for Nano Science and Technology, National Central University, Jhong-li 32001, Taiwan

²Department of Electrical Engineering, National Central University, Jhong-li 32001, Taiwan

³Department of Electrophysics, National Chiao Tung University, Hsinchu 300, Taiwan

(Received 15 September 2008; accepted 7 April 2009; published online 23 April 2009)

This work explores the origins of nonzero multiphoton emission probability for quantum dots embedded in photonic crystal nanocavities using different excitation energies to inject excitons into either the GaAs barrier or the quantum-dot excited state. The detected multiphoton events are established to arise from both the recapture of excitons and background emissions from the wetting layer tail states. The exciton emission is analyzed using rate-equation calculations, which suggest that multiphoton emission is dominated by the recapture effect. © 2009 American Institute of Physics. [DOI: 10.1063/1.3125222]

The exploitation of semiconductor self-assembled quantum dots (QDs) to develop a solid-state single photon emitter is currently of interest for quantum information applications.^{1–4} To produce on-demand single photon turnstiles, QDs were incorporated into an optical cavity to enhance the spontaneous emission (SE) rate and the photon extraction efficiency. Various monolithic optical cavities including microdisks,¹ microposts,^{2,5,6} and photonic-crystal nanocavities (PC-NCs)^{4,7} have been adopted, of which PC-NCs are the most frequently employed to enhance the SE rate because of their high quality factor (Q) and small modal volume (V_m).⁴ High-coupling-efficiency single-mode single photon emitters⁴ and ultralow-threshold self-tuned QD lasers⁸ have been demonstrated using such PC-NCs. However, the probability of unwanted multiple photon emissions is usually found to increase when the single-QD line is spectrally resonated with (or even somewhat detuned from) the PC-NC cavity modes,^{4,9} especially when electron-hole pairs are generated in barrier materials. The multiple photon emissions are attributable to the recapture of excitons in the fast radiative QDs,¹⁰ as well as to the QD background.^{5,8,9} Since multiple photon emission limits the range of applications of single photon emitters—particularly to electrically driven devices in which carriers are injected into barrier materials, the major contributions must be examined. This study explores the origins of the nonzero multiphoton emission probability from QDs that are embedded in PC-NCs, using different excitation schemes—injecting excitons into either the GaAs barrier or the QD excited state. This work shows that the detected multiphoton events involve both the recapture of excitons and background emissions from the wetting layer (WL) states. Finally, the recapture of excitons is analyzed using rate-equation-model calculations.

Self-assembled QD samples were grown on a GaAs (100) substrate by metal-organic chemical vapor deposition. After a 500-nm-thick $\text{Al}_{0.8}\text{Ga}_{0.2}\text{As}$ sacrificial layer was deposited on the substrate, a 190 nm GaAs waveguide layer with a layer of low-density ($\sim 3 \mu\text{m}^{-2}$) $\text{In}_{0.5}\text{Ga}_{0.5}\text{As}$ QDs (Ref. 11) embedded at the center was then grown. The

PC-NC used herein is the $L3$ defected cavity, which was fabricated by electron-beam lithography with air-hole period $a=300$ nm and radius $r=0.31a$.⁷

The coupling of QD emissions with the PC-NC cavity mode was examined by measuring microphotoluminescence (μPL) at liquid He temperature, using either an He–Ne laser or a Ti:sapphire laser as a pumping source. Photon correlation measurements were made using a Hanbury–Brown and Twiss setup to record the second-order correlation function $g^{(2)}(\tau)$. Both μPL and correlation measurements have been described in detail elsewhere.¹² Correlation measurements were made under pulsed excitations using a mode-locked Ti:sapphire laser, which delivered a 3 ps pulse train at 76 MHz.

Two representative PC-NCs (A and B) were utilized herein to explore the photon statistics of single QDs that resonated with, or were somewhat detuned from, the cavity mode. Figure 1 shows the μPL spectra of both cavities at different excitation powers (P). For PC-NC A, a broad band WL emission near 1.36 eV and cavity mode emission near 1.315 eV are observed. At lower P , the single exciton line (X) of the QD in this cavity was closed to 1.316 eV, which is on resonance with the cavity mode, as has been verified by power-dependence and polarization-resolved measurements.¹² The μPL spectra of PC-NC B, which is shown in Fig. 1, exhibited similar spectral features, except that the X line of the QD in this cavity is detuned from the cavity mode by about 10 meV.

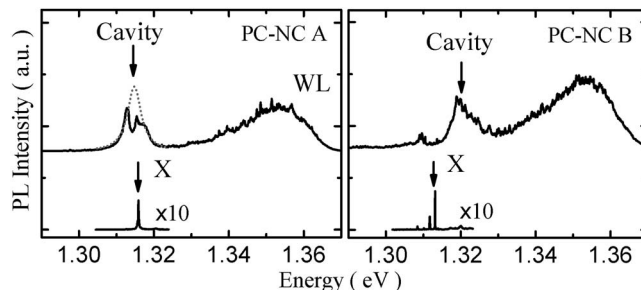


FIG. 1. The μPL spectra reveal QD exciton (X), PC-NC cavity mode and WL emissions for PC-NC A and PC-NC B at an excitation energy of 1.96 eV and pumping powers of 1.25 μW (top) and 2.5 nW (bottom).

^{a)}Electronic mail: tmhsu@phy.ncu.edu.tw.

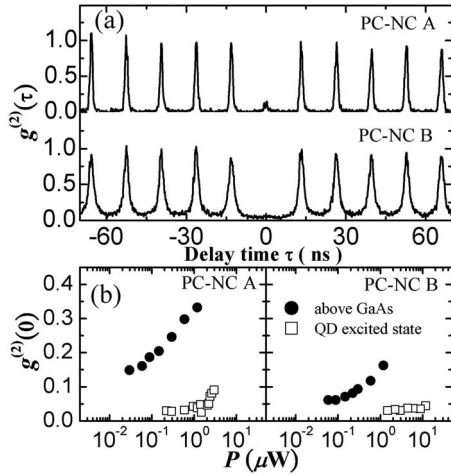


FIG. 2. (a) Second-order correlation functions $g^{(2)}(\tau)$ for PC-NC A and B at $E_{\text{ex}}=1.55$ eV. (b) Power dependence of $g^{(2)}$ at excitation energies of 1.55 eV (●) and of excited state of QD (□).

Figure 2(a) plots the measured second-order correlation functions $g^{(2)}(\tau)$ for both the PC-NC A and B under pulsed laser excitations at 1.55 eV. Despite the clear signature of photon antibunching observed at zero delay ($\tau=0$) for both cavities, some non-negligible multiphoton events were still detected, particularly for the PC-NC A, where the QD emission is on resonance with the cavity mode. For an ideal single photon emitter, $g_0^{(2)}=0$ is expected. However, the measured $g_0^{(2)}$ values for the PC-NC A (on resonance) and the PC-NC B (off resonance) were 0.15 and 0.06, respectively; both increased with P [Fig. 2(b)]. The markedly higher multiphoton probability in the case of QD-cavity resonance is attributable to the exciton recapture effect. For the above band gap excitations, excitons were first created in the GaAs barrier, followed by a fast relaxation into the WL state and then captured by the QDs. When the exciton lifetime in the QD (τ_{QD}) is short, some residual excitons remain in the WL after the QD emission. These long-lasting residual excitons would be recaptured into the QD after the recombination of the preceding exciton, causing multiphoton emissions in the same excitation cycle. This effect is expected to be stronger at higher P because of the presence of more long-lasting excitons in the WL state, in consistence with our experimental results.¹⁰

The exciton lifetimes for QDs were determined by making time-resolved PL measurements. The emission lifetimes for the QDs in PC-NC A is $\tau_{\text{QD,A}}=0.28$ ns, considerably shorter than that for QDs in the absence of PC ($\tau_{\text{QD,0}}=0.65$ ns), because of QD-cavity resonance. For PC-NC B, a slightly longer QD emission lifetime $\tau_{\text{QD,B}}=0.94$ ns was found, indicative of a suppressed SE rate into the photonic band gap owing to cavity detuning. The measured lifetime $\tau_{\text{QD,A}}$ is shorter than $\tau_{\text{QD,B}}$, indicating that recapture of excitons are more significant for the on-resonance case. However, multiple photon emission probability still occurred in an off-resonance case, implying that the multiple photon emission in our experiments was not solely due to the exciton recapture: background emission also contributes.

Since the WL behaves as an exciton reservoir during the recapture processes, optical excitation via QD excited states with energies below the WL may reduce the multiple photon emissions. Indeed, resonant excitations to the excited state of

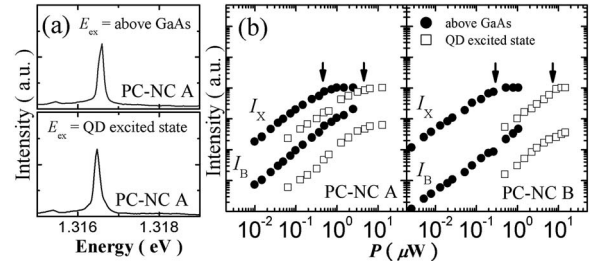


FIG. 3. (a) μPL spectra of PC-NC A, showing the superposition of X and background line shapes at $E_{\text{ex}}=1.55$ and 1.354 eV. (b) Power-dependent intensities of X (I_X) and background (I_B) at excitation energies of 1.55 eV (●) and of excited state of QD (□).

single excitons ensures the generation of only one exciton per pulse since the excited states of biexcitons or multiexcitons are a few meV's apart due to the few-particle Coulomb interactions.² To identify the QD excited states of single exciton, μPL excitation spectroscopy was performed, determining that the excited-state energies were 1.354 and 1.350 eV for the PC-NC A and B, respectively. Figure 2(b) plots the measured $g_0^{(2)}$ as a function of P for the two cavities under QD excited-state excitations. $g_0^{(2)}$ was substantially reduced for both cavities, indicative of a reduced multiphoton emission probability due to the inhibited exciton recapture effect.

The nonzero $g_0^{(2)} \sim 0.03$ at QD excited-state excitations suggest that there still have some sources of background emissions other than the recapture effect. Figure 3(a) shows the spectra of X lines taken from the PC-NC A at different excitation energies. One can see that the PL background level is almost the same for both cases, regardless of how the excitons were created, i.e., either into the GaAs barrier or the QD excited state. The background PL is very likely to arise from the emission of WL tail states⁸ as well as the other QDs. For the latter, the PL of the other QDs may couple into the spectral window of interest via phonon mediation⁵ and/or photon induced shake up process⁹ even if the emission energy of each QD is different. In our case, the major contribution to background PL is WL tail states rather than the other QDs because each PC-NC contains only two to three QDs (estimated from QD density). Figure 3(b) plots the power dependence of exciton (I_X) and background (I_B) intensities for both cavities. In which I_X saturates at $P \geq P_0$ (because of the formation of biexciton) and I_B increases persistently with P . Since the cavity has less absorption for excited-state excitation than for above-band-gap excitation, the pumping must be stronger to yield I_X and I_B signals for the former. The power dependence of the background emission ratio $\xi \equiv I_B/(I_B+I_X)$ is then demonstrated by using P_0 as the normalization factor. From Fig. 4(a), ξ depends only on the normalized pumping power (P/P_0), and which is independent of the excitation energies E_{ex} . Also, the PC-NC A had a larger ξ than PC-NC B, indicating that the cavity mode also enhances the background emission. Figure 4(a) reveals that ξ is independent of E_{ex} , despite the measured $g_0^{(2)}$ shows a strong E_{ex} dependence. Hence, the measured $g_0^{(2)}$ under excited-state excitations can be regarded as the multiphoton probability of the background emission $g_{B,0}^{(2)}$. Accordingly, as shown in Fig. 4(b), the contribution of exciton-recapture $g_{R,0}^{(2)}$ at the above-band-gap excitation can be deduced from $g_{R,0}^{(2)} = g_0^{(2)} - g_{B,0}^{(2)}$.

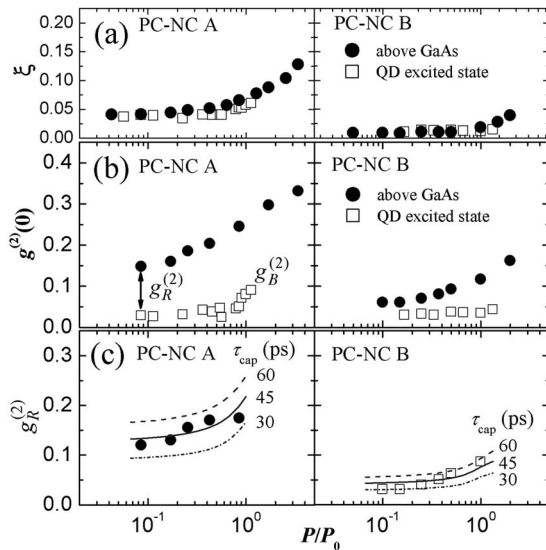


FIG. 4. (a) Normalized power dependence of background ratios ξ at excitation energies of 1.55 eV (\bullet) and of excited state of QD (\square). (b) Normalized power dependence of $g_R^{(2)}$ at excitation energies of 1.55 eV (\bullet) and of excited state of QD (\square). (c) Normalized power dependence of measured (symbols) and calculated (lines) $g_{R,0}^{(2)}$, with $\tau_0=0.57$ ns (from TRPL) in Eq. (1).

The exciton recapture $g_{R,0}^{(2)}$ can be analyzed using rate-equation calculations. If the exciton number at WL is n_{WL} , while those populating at the QD's empty state, exciton state and biexciton state are n_0 , n_X , and n_{2X} , respectively. For $n_0(t) + n_X(t) + n_{2X}(t) = 1$, the time evolution of this system is expressed as¹⁰

$$\begin{aligned} \frac{dn_{WL}}{dt} &= -\frac{n_{WL}}{\tau_{cap}}(n_0 + n_X) - \frac{n_{WL}}{\tau_0}, \\ \frac{dn_X}{dt} &= \frac{n_{WL}}{\tau_{cap}}n_0 - \frac{n_{WL}}{\tau_{cap}}n_X - \frac{n_X}{\tau_X} + \frac{n_{2X}}{\tau_{2X}}, \\ \frac{dn_{2X}}{dt} &= \frac{n_{WL}}{\tau_{cap}}n_X - \frac{n_{2X}}{\tau_{2X}}, \end{aligned} \quad (1)$$

where τ_X , τ_{2X} , and τ_0 are recombination lifetime of exciton, biexciton, and exciton in the WL state, respectively, and τ_{cap} is the capture time of excitons into the QDs from WL. After exciton recombines, the QD is at empty state, and $n_0=1$. Then, $g_{R,0}^{(2)}$ is given by

$$g_{R,0}^{(2)} = \frac{\int \int n_X(t)n_X(t+\tau)dt d\tau}{[\int n_X(t)dt]^2}. \quad (2)$$

Figure 4(c) plots the calculated power-dependent $g_{R,0}^{(2)}$ for PC-NC A and B,¹³ and reveals that the calculations agree closely with the measurements, confirming that the measured $g_{R,0}^{(2)}$ is dominated by exciton recapture rather than other possible mechanisms.^{2,6} The best fitting τ_{cap} for PC-NC A and B is about 45 ps, which is comparable to values presented elsewhere (10–40 ps).¹⁴ The slightly longer capture time in this work may arise from the low QD density in the samples.¹⁵ The calculations also indicate that τ_{cap} is an important parameter for $g_{R,0}^{(2)}$. At a fixed n_{WL} , a shorter τ_{cap} can result in a lower $g_{R,0}^{(2)}$ because the biexciton population increases with the reducing τ_{cap} , which leads to a much faster n_{WL} decay rate than τ_{OD}^{-1} . Although a reliable means of controlling τ_{cap} is

yet available, applying an electric field⁶ or increasing the temperature¹⁵ may be help to reduce τ_{cap} .

In summary, the origins of the nonzero multiphoton emission probability for QDs embedded in PC-NCs were investigated. Above barrier excitations usually lead to a considerable multiphoton probability, that arises from both the recapture of excitons and background emission. Excitations via the QD excited state substantially inhibit exciton recapture and the detected multiphoton events can in principle be attributable to the background emissions from WL tail states. The effect of exciton recapture is analyzed using rate equation calculations. This study suggests that exciton recapture can be suppressed by reducing the capture time of excitons into the QDs, which suppression is important to the quality control of a single photon emitter—especially the electrically driven single photon emitter, in which the electrons and holes are injected from buffer layers.

This work was supported by the National Science Council of the Republic of China under Grant No. NSC 96-2112-M-008-019-MY3.

¹P. Michler, A. Kiraz, C. Becher, W. V. Schoenfeld, P. M. Petroff, L. Zhang, E. Hu, and A. Imamoglu, *Science* **290**, 2282 (2000).

²C. Santori, D. Fattal, J. Vučković, G. S. Solomon, Y. Dale, and Y. Yamamoto *Phys. Rev. Lett.* **86**, 1502 (2001); C. Santori, D. Fattal, J. Vučković, G. S. Solomon, E. Waks, and Y. Yamamoto, *Phys. Rev. B* **69**, 205324 (2004).

³Z. Yuan, B. E. Kardynal, R. M. Stevenson, A. J. Shields, C. J. Lobo, K. Cooper, N. S. Beattie, D. A. Ritchie, and M. Pepper, *Science* **295**, 102 (2002).

⁴S. Laurent, S. Varoutsis, L. Le Gratiet, A. Lemaître, I. Sagnes, F. Raineri, A. Levenson, I. Robert-Philip, and I. Abram *Appl. Phys. Lett.* **87**, 163107 (2005); D. Englund, D. Fattal, E. Waks, G. Solomon, B. Zhang, T. Nakaoka, Y. Arakawa, Y. Yamamoto, and J. Vučković, *Phys. Rev. Lett.* **95**, 013904 (2005); W.-H. Chang, W.-Y. Chen, H.-S. Chang, T.-P. Hsieh, J.-I. Chyi, and T.M. Hsu, *ibid.* **96**, 117401 (2006); K. Hennessy, A. Badolato, M. Winger, D. Gerace, M. Atatüre, S. Gulde, S. Fält, E. L. Hu, and A. Imamoglu, *Nature (London)* **445**, 896 (2007).

⁵D. Press, S. Götzinger, S. Reitzenstein, C. Hofmann, A. Löffler, M. Kamp, A. Forchel, and Y. Yamamoto, *Phys. Rev. Lett.* **98**, 117402 (2007).

⁶S. Strauf, N. G. Stoltz, M. T. Rakher, L. A. Coldren, P. M. Petroff, and D. Bouwmeester, *Nat. Photonics* **1**, 704 (2007).

⁷W.-Y. Chen, H.-S. Chang, T. M. Hsu, T.-P. Hsieh, and J.-I. Chyi, *Appl. Phys. Lett.* **90**, 211114 (2007).

⁸S. Strauf, K. Hennessy, M. T. Rakher, Y.-S. Choi, A. Badolato, L. C. Andreani, E. L. Hu, P. M. Petroff, and D. Bouwmeester, *Phys. Rev. Lett.* **96**, 127404 (2006).

⁹M. Kaniber, A. Laucht, A. Neumann, J. M. Villas-Bôas, M. Bichler, M.-C. Amann, and J. J. Finley, *Phys. Rev. B* **77**, 161303 (2008).

¹⁰E. Peter, S. Laurent, J. Bloch, J. Hours, S. Varoutsis, I. Robert-Philip, A. Beveratos, A. Lemaître, A. Cavanna, G. Patriarche, P. Senellart, and D. Martrou *Appl. Phys. Lett.* **90**, 223118 (2007); E. Peter, S. Laurent, J. Bloch, J. Hours, S. Varoutsis, D. Martrou, I. Robert-Philip, A. Beveratos, A. Lemaître, A. Cavanna, G. Patriarche, and P. Senellart, *Phys. Status Solidi C* **5**, 2520 (2008).

¹¹T.-P. Hsieh, H.-S. Chang, W.-Y. Chen, W.-H. Chang, T. M. Hsu, N.-T. Yeh, W.-J. Ho, P.-C. Chiu, and J.-I. Chyi, *Nanotechnology* **17**, 512 (2006).

¹²W.-H. Chang, H.-S. Chang, W.-Y. Chen, T. M. Hsu, T.-P. Hsieh, J.-I. Chyi, and N.-T. Yeh, *Phys. Rev. B* **72**, 233302 (2005).

¹³For a given P , $n_{WL}(0)$ can be estimated by $n_{WL}(0) = (\alpha P T_L / E_{ex}) \times (A_{cavity} / A_{laser}) (1 / n_{QD})$, where $\alpha=0.05$ is the absorption of GaAs, T_L is the period of laser, A_{cavity} (0.25 μm^2) and A_{laser} (19.6 μm^2) are the areas of the cavity and the laser, respectively, E_{ex} is the excitation energy of the laser, and $n_{QD}=3$ is the number of QDs in the cavity.

¹⁴K. Mukai, N. Ohtsuka, H. Shoji, and M. Sugawara *Appl. Phys. Lett.* **68**, 3013 (1996); R. Heitz, M. Veit, N. N. Ledentsov, A. Hoffmann, D. Bimberg, V. M. Ustinov, P. S. Kop'ev, and Zh. I. Alferov, *Phys. Rev. B* **56**, 10435 (1997); Yu. I. Mazur, B. L. Liang, Zh. M. Wang, D. Guzun, G. J. Salamo, G. G. Tarasov, and Z. Ya. Zhuchenko, *J. Appl. Phys.* **100**, 054316 (2006).

¹⁵S. Marcinkevičius, and R. Leon, *Appl. Phys. Lett.* **76**, 2406 (2000).